Coordination Polymers of $Co(NCS)_2$ with Pyrazine and 4,4′-Bipyridine: Syntheses and Structures

Jian Lu, Tasneem Paliwala, Shiao C. Lim, Carolyn Yu, Tianyan Niu, and Allan J. Jacobson*

Department of Chemistry, University of Houston, Houston, Texas 77204-5641

Received September 18, 1996[⊗]

Three compounds were obtained from the reactions of $Co(NCS)_2$ with pyrazine and 4,4′-bipyridine in different solvents: $Co(NCS)_2(pyz)_2$ (**1**) has a 2D sheet structure, monoclinic, *C*2/*m*, $a = 10.039(2)$ Å, $b = 10.382(2)$ Å, $c = 7.190(1)$ Å, $\beta = 118.64(1)°$, $Z = 2$; $Co(NCS)_2(H_2O)_2$(4,4′-bipy)·4,4′-bipy (**2**) has linear Co−bipy−Co chains connected by hydrogen bonds between H_2O and noncoordinated 4,4′-bipy molecules to form stair type sheets, triclinic, $P\bar{1}$, $a = 7.450(1)$ Å, $b = 9.020(1)$ Å, $c = 10.122(1)$ Å, $\alpha = 107.74(1)°$, $\beta = 104.02(1)°$, $\gamma = 97.16(1)°$, $Z = 1$; $Co(NCS)_2$(4,4′-bipy)$_2$·2$(CH_3CH_2)_2O$ (**3**) has ether molecules intercalated between layers formed by $Co(NCS)_2$ and coordinated 4,4′-bipyridine ligands, monoclinic, *P*2/*c*, $a = 11.483(2)$ Å, $b = 11.397(3)$ Å, $c = 13.609(1)$ Å, $\beta = 107.55(1)°$, $Z = 2$. Compounds **2** and **3** thermally decompose to form the same products. The identities of the decomposition products are discussed.

Introduction

The formation of open framework structures based on coordination chemistry that mimic zeolite or other microporous solids was investigated recently by several groups.[1−4] The concept of crystal engineering has been used to rationally design 2D and 3D polymer structures.[5] Pyrazine and 4,4′-bipyridine are good candidates for molecular building blocks because of their rodlike rigidity and length. One of the issues of particular interest is to establish the conditions that determine the formation of open structures rather than interpenetrated lattices. In the polymeric structures reported that contain pyrazine and 4,4′-bipyridine, several factors influence the specific framework structure that is formed. For example, the coordination of solvent (water) molecules in the compound $[Zn(4,4'\text{-bipy})_2(H_2O)_2]SiF_6$ results in an interpenetrated sheet structure,[6] while under nonaqueous conditions, a porous solid $[Zn(4,4'\text{-bipy})_2(SiF_6)]_n$·*x*DMF is obtained.[7] Similarly, a dramatic difference is observed between the double-layer structure of the solvent-inclusion compound $[Ag(pyz)_2][Ag_2(pyz)_5](PF_6)_3$·2S (S = CH_2Cl_2, $CHCl_3$, CCl_4)[8] and the layer structure of the solvent-free compound $[Ag(pyz)_2](PF_6)$.[9] In the same solvent, the specific counterion can also influence the final structure. For example, changing the counterion from PF_6^- to SbF_6^- changes the structure from the double layer structure of Ag−pyrazine−PF_6 to the 3D noninterpenetrating cubic framework of $Ag(pyz)_3SbF_6$.[8] The counterion effect is also apparent in a comparison of the 2D undulated sheet structure of $[Ag(pyz)_2](PF_6)$[9] and the interpenetrated 3D structure of $[Ag_2(pyz)_3](BF_4)_2$.[10]

As expected, the specific oxidation state and the coordination preference of the metal cation play an important role in determining the final polymer structure. Thus Cu^{2+} is normally octahedrally coordinated (distorted) and forms square 2D networks with pyrazine or substituted pyrazine[11] or interpenetrated 2D networks with 4,4′-bipyridine.[5a] On the other hand, Cu^+ can adopt various types of coordination modes. Tetrahedrally coordinated Cu^+ cations form 3D or 2D networks with substituted pyrazine or 4,4′-bipyridine.[11a,12] Cu^+ cations may also be trigonally coordinated by 4,4′-bipyridine, pyrazine, or substituted pyrazines, forming 3D networks or 2D layers containing six-membered rings.[12ace,13] Ag^+ is observed in an even wider range of coordination environments (e.g. linear,[10,14] trigonal,[10] tetrahedral,[9,10,15] square-planar,[8] square-pyramidal,[8]

* Author to whom correspondence should be addressed.

[⊗] Abstract published in *Advance ACS Abstracts,* February 1, 1997.

(1) See, e.g.: (a) Abrahams, B. F.; Hoskins, B. F.; Michall, D. M.; Robson, R. *Nature* **1994**, *369*, 727. (b) Hoskins, B. F.; Robson, R. *J. Am. Chem. Soc.* **1990**, *112*, 1546.

(2) See, e.g.: (a) Schwarz, P.; Siebel, E.; Fischer, R. D.; Apperley, D. C.; Davies, N. A.; Harris, R. K. *Angew. Chem., Int. Ed. Engl.* **1995**, *34*, 1197. (b) Behrens, U.; Brimah, A. K.; Soliman, T. M.; Fischer, R. D.; Apperley, D. C.; Davies, N. A.; Harris, R. K. *Organometallics* **1992**, *11*, 1718 and references therein.

(3) See, e.g.: (a) Kitazawa, T.; Nishikiori, S.; Iwamoto, T. *J. Chem. Soc., Dalton Trans.* **1994**, 3695. (b) Park, K. M.; Iwamoto, T. *J. Inclusion Phenom.* **1991**, *11*, 397.

(4) (a) Lu, J.; Harrison, W. T. A.; Jacobson, A. J. *Angew. Chem., Int. Ed. Engl.* **1995**, *34*, 2557. (b) Yaghi, O. M.; Li, G.; Li, H. *Nature* **1995**, *378*, 703. (c)Yaghi, O. M.; Li, G. *Angew. Chem., Int. Ed. Engl.* **1995**, *34*, 207. (d) Gardner, G. B.; Venkataraman, D.; Moore, J. S.; Lee, S. *Nature* **1995**, *374*, 792. (e) Hirsch, K. A.; Venkataraman, D.; Wilson, S. R.; Moore, J. S.; Lee, S. *J. Chem. Soc., Chem. Commun.* **1995**, 2199. (f) Gardner, G. B.; Kiang, Y. H.; Lee, S.; Asgaonkar, A.; Venkataraman, D. *J. Am. Chem. Soc.* **1996**, *118*, 6946. (g) Fujita, M.; Oguro, D.; Milyazawa, M.; Oka, H.; Yamaguchi, K.; Ogura, K. *Nature* **1995**, *378*, 469.

(5) See, e.g.: (a) Robson, R.; Abrahams, B. F.; Batteen, S. R.; Gable, R. W.; Hoskins, B. F.; Liu, J. *Supramolecular Architecture*; Bein, T., Ed.; ACS Symposium Series 499; American Chemical Society: Washington, DC, 1992; Chapter 19. (b) Zaworotko, M. J. *Chem. Soc. Rev.* **1994**, 283.

(6) Gable, R. W.; Hoskins, B. F.; Robson, R. *J. Chem. Soc., Chem. Commun.* **1990**, 1677.

(7) Subramanian, S.; Zaworotko, M. J. *Angew. Chem., Int. Ed. Engl.* **1995**, *34*, 2127.

(8) Carlucci, L.; Ciani, G.; Proserpio, D. M.; Sironi, A. *Angew. Chem., Int. Ed. Engl.* **1995**, *34*, 1895.

(9) Carlucci, L.; Ciani, G.; Proserpio, D. M.; Sironi, A. *Inorg. Chem.* **1995**, *34*, 5698.

(10) Carlucci, L.; Ciani, G.; Proserpio, D. M.; Sironi, A. *J. Am. Chem. Soc.* **1995**, *117*, 4562.

(11) (a) Halasyamani, P.; Heier, K. R.; Willis, M. J.; Stern, C. L.; Poppelmeier, K. R. *Z. Anorg. Allg. Chem.* **1996**. *622*, 479. (b) Darriet, J.; Haddad, M. S.; Duesler, E. N.; Hendrickson, D. N. *Inorg. Chem.* **1979**, *18*, 2679. (c) Haynes, J. S.; Rettig, S. J.; Sams, J. R.; Thompson, R. C.; Trotter, J. *Can. J. Chem.* **1987**, *65*, 420. (d) Otieno, T.; Rettig, S. J.; Thompson, R. C.; Trotter, J. *Inorg. Chem.* **1993**, *32*, 4384.

(12) (a) MacGillivray, L. R.; Subramanian, S.; Zaworotko, M. J. *J. Chem. Soc., Chem. Commun.* **1994**, 1325. (b) Lumme, P.; Lindroos, S.; Lindell, E. *Acta Crystallogr.* **1987**, *C43*, 2053. (c) Otieno, T.; Rettig, S. J.; Thompson, R. C.; Trotter, J. *Inorg. Chem.* **1993**, *32*, 1607. (d) Kitagawa, S.; Munakata, M.; Tanimura, T. *Inorg. Chem.* **1992**, *31*, 1714. (e) Kitagawa, S.; Kawata, S.; Kondo, M.; Nozaka, Y.; Munakata, M. *Bull. Chem. Soc. Jpn.* **1993**, *66*, 3387.

(13) (a) Yaghi, O. M.; Li, H. *J. Am. Chem. Soc.* **1995**, *117*, 10401. (b) Turnbull, M. M.; Pon, G.; Willett, R. D. *Polyhedron* **1991**, *10*, 1835.

S0020-1669(96)01158-5 CCC: $14.00 © 1997 American Chemical Society

and octahedral[8]) when bonded to pyrazine or 4,4′-bipyridine ligands. The differences between the coordination preferences of Ag^+ and Cu^+ ions can be seen by comparing the structures formed with 4,4′-bipyridine as the ligand and NO_3^- as the counterion. Thus Ag^+ is linearly coordinated in the T-shaped Ag(4,4′-bipy)NO_3 structure[14] and Cu^+ is found in a trigonal planar environment in Cu(4,4′-bipy)$_{1.5}NO_3(H_2O)_{1.5}$.[13a] In contrast, Cd^{2+} is octahedrally coordinated in the 2D square network structure of [Cd(4,4′-bipy)$_2$]$(NO_3)_2$.[16] The difference between the preferred coordination environments for Ag^+ and Cu^+ is also apparent in the structures of [Ag(pyz)$_2$][Ag$_2$(pyz)$_5$]$(PF_6)_3$·$2CH_2Cl_2$, (square-pyramidal and square-planar Ag^+)[8] and [Cu(pyz)$_{1.5}$(CH_3CN)](PF_6)·$0.5C_3H_6O$ (tetrahedral Cu^+).[12d] Variations in the Ag^+/ligand ratio in the reaction of $AgBF_4$ with pyrazine also results in different structure types.[10]

As apparent from the brief review above, the formation of coordination polymers of group IB and IIB metal ions with pyrazine and 4,4′-bipyridine ligands has been studied in some detail. In contrast, the formation of polymers with other transition metal ions has been less well investigated. In the present work, we report results of the reactions of $Co(NCS)_2$ with pyrazine and 4,4′-bipyridine. In different solvent systems, three new compounds are formed: $Co(NCS)_2(pyz)_2$ (**1**), $Co(NCS)_2(H_2O)_2$(4,4′-bipy)·4,4′-bipy (**2**), and $Co(NCS)_2$(4,4′-bipy)$_2$·$2(CH_3CH_2)_2O$ (**3**). The new compounds **1**−**3** do not form interpenetrating lattices, and as in other systems, we find that the specific solvent plays an important role in determining the final polymer structure.

Experimental Section

All reagents were obtained from Aldrich and used as received. Infrared data were collected on a Galaxy FTIR 5000 series spectrometer using the KBr pellet method. X-ray powder diffraction measurements were carried out using a Scintag XDS 2000 automated powder diffractometer. The Lazy-Pulverix program[17] was used to simulate powder patterns from the single-crystal X-ray data. Thermogravimetric data were collected on a DuPont 9900 TG analyzer in flowing nitrogen at a heating rate of 10 °C/min.

$Co(NCS)_2(pyz)_2$ (1). An acetone solution (15 mL) of pyrazine (0.405 g, 5.0 mmol) was slowly diffused into an aqueous solution (10 mL) of $Co(NCS)_2$ (0.434 g, 2.5 mmol). Orange block crystals of **1** were formed in 1 week. In other solvents (e.g., ethanol, methanol, THF, and acetonitrile), crystalline material was also obtained, but the acetone/water combination gave the best-quality crystals. The typical yield was 80% based on $Co(NCS)_2$. The compound is not soluble in water or common organic solvents. The purity of the bulk sample was checked by X-ray powder diffraction. Bulk samples gave the same X-ray powder pattern as that simulated from the single-crystal X-ray structure data. IR: 3441 m, 3119 w, 3053 w, 2874 w, 2363 w, 2066 vs, 2014 w, 1624 m, 1419 w, 1416 s, 1163 m, 1126 m, 1115 w, 1055 s, 970 w, 801 m, 486 w, 463 s cm^{-1}.

$Co(NCS)_2(H_2O)_2$(4,4′-bipy)·4,4′-bipy (2). A 0.315 g (2.0 mmol) sample of 4,4′-bipy dissolved in 15 mL of ethanol was layered on top of an aqueous solution (10 mL) of $Co(NCS)_2$ (0.163 g, 0.93 mmol). In about 1 week, light orange plate crystals of **2** were formed. After diffusion was completed, the product was filtered off and dried under vacuum, giving 0.374 g of product. The yield was 79% based on $Co(NCS)_2$. **2** does not dissolve in common organic solvents or water. X-ray powder data for bulk samples were compared with the pattern simulated from the single-crystal structure and shown to be those of a single phase. IR: 3403 s, 3067 w, 3038 w, 2884 m, 2098 vs, 1942 w, 1688 w, 1607 s, 1537 m, 1503 m, 1404 m, 1319 w, 1217 m, 1068 m, 999 w, 808 s, 729 w, 633 m, 471 w cm^{-1}.

$Co(NCS)_2$(4,4′-bipy)$_2$·$2(CH_3CH_2)_2O$ (3). The reaction was carried out in the same way as for **2** except that ether was used instead of ethanol. Two types of crystals were formed in the same reaction tube. From around the solution interface were recovered some orange-red square crystals of **3**, while in the lower part of the tube, crystals of **2** (identity was checked by determining the unit cell by X-ray single-crystal diffraction) were formed. The yield of crystals of **3** varied from 30% to 70% of the total weight of crystals formed. The use of dried ether (for 4,4′-bipy) and ethanol (for $Co(NCS)_2$) solvents resulted in the formation of a single phase of **3**. **3** is not soluble in water or common organic solvents and loses ether immediately after the crystals are removed from the mother liquor. IR: 3460 w, 3040 w, 2868 w, 2064 vs, 1605 s, 1534 m, 1487 m, 1410 m, 1321 w, 1217 m, 1070 m, 1006 w, 804 m, 731 w, 629 m, 574 w, 536 w, 482 w cm^{-1}.

X-ray Crystallography. For **1**, a dark red square block crystal with dimensions of 0.25 × 0.22 × 0.18 mm^3 was covered with epoxy and glued to the top of a glass fiber. Fourteen reflections in the range 17° < 2θ < 28° were located by using a semiautomatic search routine and centered afterward. Least-squares refinement of these 14 reflections resulted in a monoclinic cell. The Laue symmetry 2/*m* was confirmed by checking the intensities of the equivalent reflections, i.e. *hkl*, $h\bar{k}l$, $\bar{h}k\bar{l}$, and $\bar{h}\bar{k}l$. Intensity data were collected on an Enraf-Nonius CAD-4 diffractometer using the 2θ−ω scan mode in the range 4° < 2θ < 46°. Orientation and intensity changes were monitored with two standard reflections during the data collection. An absorption correction based on ψ scans (minimum 1.16, maximum 1.30) was applied to the data during data reduction. An intensity decay correction was not necessary. Space groups *C*2, *Cm*, and *C*2/*m* were consistent with the systematic absence conditions. The initial structure model was developed from the Patterson map provided by the SHELXS-86 program[18] in space group *Cm*, and the other atom positions were located from repeated Fourier difference maps during the refinement. The structure was refined on F^2 using full-matrix least-squares procedures for all data (SHELXL-93).[19] A symmetry check at the later stage of refinement indicated that *C*2/*m* (No. 12) was the correct choice and was used for the final refinement. After all non-hydrogen atoms were refined, hydrogen atoms were located from a difference Fourier synthesis. Positional parameters of hydrogen atoms were refined without constraints.

The data collection and refinement of the structures of **2** and **3** were carried out similarly. For **2**, a light orange plate crystal of dimensions 0.17 × 0.10 × 0.51 mm^3 was used. Twenty-five reflections were centered on a triclinic cell. Intensity data were collected using a 2θ−ω scan mode in the range 4° < 2θ < 50°. An absorption correction based on ψ scans (minimum 1.00, maximum 1.24) was applied to the data during data reduction. The structure was determined and refined in space group $P\bar{1}$. Hydrogen atom positions were located from a difference Fourier synthesis and were refined without constraints.

For **3**, crystals were taken from the reaction tube with mother liquor using a pipet and placed in a small dish. An orange-red square block crystal, dimensions 0.32 × 0.32 × 0.50 mm^3, was quickly dipped into freshly mixed epoxy and attached to the top of a glass fiber. Twenty-five reflections in the range 20° < 2θ < 25° were centered on a monoclinic cell. Intensity data were collected using the ω scan mode in the range 4° < 2θ < 50°. An absorption correction based on ψ scans (minimum 1.34, maximum 1.48) was applied to the data during data reduction. Space groups *Pc* and *P*2/*c* were consistent with the systematic absence conditions. *P*2/*c* (No. 13) was chosen and confirmed by successful structure refinement. The solvent molecule (ether) was refined isotropically. Space group *Pc* was also tested and was excluded because a stable refinement could not be obtained. No hydrogen atoms were located. The relatively high *R* values may due to the partial loss of ether molecules during the crystal mounting.

Crystallographic data for **1**−**3** are summarized in Table 1.

(14) Yaghi, O. M.; Li, H. *J. Am. Chem. Soc.* **1996**, *118*, 295.
(15) Carlucci, L.; Ciani, G.; Proserpio, D. M.; Sironi, A. *J. Chem. Soc., Chem. Commun.* **1994**, 2755.
(16) Fujita, M.; Kwon, Y. J.; Washizu, S.; Ogura, K. *J. Am. Chem. Soc.* **1994**, *116*, 1151.
(17) Yvon, K.; Jeitschko, W.; Parthe, E. *J. Appl. Crystallogr.* **1977**, *10*, 73.
(18) Sheldrick, G. M. *SHELXS-86 User Guide*; University of Gottingen: Gottingen, Germany, 1986.
(19) Sheldrick, G. M. *SHELX93*: *Program for crystal structure refinement*; University of Gottingen: Gottingen, Germany, 1993.

Table 1. Crystal Data and Structure Refinement for $Co(NCS)_2(pyz)_2$ (**1**), $Co(NCS)_2(H_2O)_2(4,4'\text{-bipy})\cdot 4,4'\text{-bipy}$ (**2**), and $Co(NCS)_2(4,4'\text{-bipy})_2\cdot 2(CH_3CH_2)_2O$ (**3**)

	1	**2**	**3**
formula	$C_{10}H_8CoN_6S_2$	$C_{22}H_{20}CoN_6O_2S_2$	$C_{30}H_{36}CoN_6O_2S_2$
fw	335.27	523.49	635.70
a (Å)	10.039(2)	7.450(1)	11.483(2)
b (Å)	10.382(2)	9.020(1)	11.397(3)
c (Å)	7.190(1)	10.122(1)	13.609(1)
α (deg)	90	107.74(1)	90
β (deg)	118.64(1)	104.02(1)	107.55(1)
γ (deg)	90	97.16(1)	90
V (Å^3)	657.7(2)	613.9(1)	1698.1(6)
Z	2	1	2
space group	*C*2/*m* (No. 12)	$P\bar{1}$ (No. 2)	*P*2/*c* (No. 13)
T (°C)	25(2)	25(2)	25(2)
λ(Mo Kα)	0.710 73	0.710 73	0.710 73
ρ_{calc} (g/cm^3)	1.693	1.416	1.243
μ(Mo Kα) (mm^{-1})	1.615	0.900	0.662
R(all data)[a]	0.0304	0.0418	0.0698
w*R*2(all data)[b]	0.0889	0.1234	0.2171

[a] $R = \sum||F_o| - |F_c||/\sum|F_o|$. [b] $wR2 = [\sum w(F_o^2 - F_c^2)^2/\sum w(F_o^2)^2]^{1/2}$, $w = [\sigma^2(F_o)^2 + (0.1(\max(0,F_o^2) + 2F_c^2)/3)^2]^{-1}$.

Table 2. Atomic Coordinates ($\times 10^4$) and Equivalent Isotropic Displacement Parameters (Å^2 $\times$ 10^3) for **1**

	x	*y*	*z*	*U*(eq)[a]
Co	0	0	0	21(1)
S	3522(2)	0	7337(2)	55(1)
N(1)	1550(2)	1532(2)	63(3)	25(1)
N(2)	1093(4)	0	3248(5)	30(1)
C(1)	2091(5)	0	4971(6)	28(1)
C(2)	2940(3)	1734(3)	1657(5)	38(1)
C(3)	1126(3)	2313(3)	−1587(4)	38(1)

[a] *U*(eq) is defined as one-third of the trace of the orthogonalized $\boldsymbol{U}_{ij}$ tensor.

Table 3. Atomic Coordinates ($\times 10^4$) and Equivalent Isotropic Displacement Parameters (Å^2 $\times$ 10^3) for **2**

	x	*y*	*z*	*U*(eq)[a]
Co	0	0	0	33(1)
S	4325(1)	1190(2)	−2617(1)	84(1)
O	1337(3)	−1726(3)	563(2)	45(1)
N(21)	2008(3)	1858(2)	1858(2)	36(1)
C(22)	2275(4)	1788(3)	3186(3)	39(1)
C(23)	3432(4)	2966(3)	4427(3)	38(1)
C(24)	4399(3)	4340(3)	4344(2)	32(1)
C(25)	4129(4)	4412(3)	2950(3)	42(1)
C(26)	2956(4)	3166(3)	1764(3)	43(1)
N(31)	1824(3)	258(3)	−1236(2)	46(1)
C(32)	2864(4)	658(4)	−1791(3)	44(1)
N(61)	−451(5)	3113(4)	−2447(3)	65(1)
C(62)	−1336(6)	2406(4)	−3863(5)	69(1)
C(63)	−1199(6)	3084(4)	−4904(4)	59(1)
C(64)	−81(4)	4609(4)	−4463(3)	46(1)
C(65)	818(5)	5345(5)	−2997(4)	58(1)
C(66)	604(6)	4554(5)	−2040(4)	66(1)

[a] *U*(eq) is defined as one-third of the trace of the orthogonalized $\boldsymbol{U}_{ij}$ tensor.

Results and Discussion

Structure. Atomic coordinates and equivalent isotropic displacement parameters for **1**, **2**, and **3** are listed in Tables 2−4, respectively. Selected bond distances and angles for **1**, **2**, and **3** are given in Table 5.

The reported 2D coordination polymers formed by pyrazine or substituted pyrazine ligands bridging metal centers are mainly copper and silver compounds. Structure types commonly observed: (1) square nets, for example $[Ag(pyz)_2Ag_2(pyz)_5](PF_6)_3$,[8] $Fe(pyz)_2(NCS)_2$,[20] $CoCl_2(pyz)_2$,[21] and all reported Cu(II) pyrazine compounds;[11] (2) nets formed by six-membered rings of metal ions bridged by pyrazine ligands, for example $[Ag_2(pyz)_3](BF_4)_2$[10] and all Cu(I) pyrazine compounds;[11a,12a,12c−e,13b] (3) the nonplanar square net formed by $[Ag(pyz)_2](PF_6)$.[9] Of the two-dimensional networks reported with pyrazine bridging ligands, only $Cu_2(pyz)_3SiF_6$[12a] has an interpenetrated structure.

Table 4. Atomic Coordinates ($\times 10^4$) and Equivalent Isotropic Displacement Parameters (Å^2 $\times$ 10^3) for **3**

	x	*y*	*z*	*U*(eq)[a]
Co	0	2003(1)	2500	29(1)
N(4)	0	3907(4)	2500	37(1)
S(2)	−2261(2)	1750(2)	−1020(1)	84(1)
N(1)	1917(3)	1978(3)	2508(3)	36(1)
N(2)	−544(3)	2046(3)	901(3)	42(1)
C(14)	4357(4)	1910(4)	2502(3)	40(1)
C(2)	−1242(4)	1917(3)	102(4)	40(1)
N(3)	0	104(4)	2500	39(1)
C(34)	0	7647(5)	2500	40(1)
C(16)	2821(4)	2422(5)	3290(4)	53(1)
C(13)	3435(4)	1443(5)	1691(4)	59(1)
C(32)	−677(4)	−520(4)	1693(4)	53(1)
C(12)	2234(4)	1494(5)	1742(4)	52(1)
C(15)	4037(4)	2388(5)	3319(4)	53(1)
C(33)	−698(5)	8278(4)	1660(4)	56(1)
C(44)	0	6353(5)	2500	42(1)
C(42)	294(4)	4519(4)	1775(3)	47(1)
C(43)	300(5)	5731(3)	1746(4)	48(1)
O	6392(6)	6896(5)	468(4)	109(2)[b]
C(62)	6681(9)	5700(9)	540(7)	126(3)[b]
C(63)	6015(9)	7266(9)	1315(8)	120(3)[b]
C(61)	7088(11)	5343(10)	−396(9)	141(4)[b]
C(64)	5814(10)	8603(10)	1200(9)	143(4)[b]

[a] *U*(eq) is defined as one-third of the trace of the orthogonalized $\boldsymbol{U}_{ij}$ tensor. [b] U_{iso} (Å^2 $\times$ 10^3).

Table 5. Selected Bond Distances (Å) and Angles (deg) for **1**−**3**

	$Co(NCS)_2(pyz)_2$ (**1**)		
Co−N(1)	2.210(2)	Co−N(2)	2.050(3)
N(2)−C(1)	1.161(5)	C(1)−S	1.617(4)
N(1)−Co−N(1)′	92.0(1)	C(1)−N(2)−Co	158.8(3)
N(2)−Co−N(2)′	180	N(2)−Co−N(1)	89.40(9)
N(2)−C(1)−S	178.0(3)		
	$Co(NCS)_2(H_2O)_2(4,4'\text{-bipy})\cdot 4,4'\text{-bipy}$ (**2**)		
Co−N(21)	2.162(2)	Co−N(31)	2.095(2)
N(31)−C(32)	1.145(4)	C(32)−S	1.634(3)
Co−O	2.096(2)		
N(31)−Co−N(31)′	180	N(31)−Co−N(21)	88.95(8)
N(31)−Co−O	90.1(1)	O−Co−N(21)	89.69(8)
C(32)−N(31)−Co	168.9(2)	N(31)−C(32)−S	178.6(3)
	$Co(NCS)_2(4,4'\text{-bipy})_2\cdot 2(CH_3CH_2)_2O$ (**3**)		
Co−N(1)	2.199(3)	Co−N(3)	2.164(4)
Co−N(4)	2.171(5)	Co−N(2)	2.076(4)
N(2)−C(2)	1.149(6)	C(2)−S(2)	1.631(5)
N(2)−Co−N(2)′	177.3(2)	N(2)−Co−N(1)	90.6(1)
N(1)−Co−N(1)′	178.5(2)	N(3)−Co−N(4)	180.0
C(2)−N(2)−Co	153.2(3)	N(2)−C(2)−S(2)	178.4(4)

The structure of **1** belongs to type 1 and is isostructural with $Fe(pyz)_2(NCS)_2$,[20] the structure of which is fully described. **1** also has the same general type of structural arrangement as $CoCl_2(pyz)_2$.[21] Figure 1a shows the local coordination of the cobalt center, and Figure 1b shows the extended structure of **1**. In **1**, pyrazine groups bridge cobalt(II) centers to form layers. The NCS groups occupy the axial positions. The layers are stacked along the *c* axis with an interlayer separation of 6.31

(20) Real, J. A.; Munno, G. D.; Munoz, M. C.; Julve, M. *Inorg. Chem.* **1991**, *30*, 2701.
(21) Carreck, P. W.; Goldstein, M.; McPartlin, E. M.; Unsworth, W. D. *Chem. Commun.* **1971**, 1634.

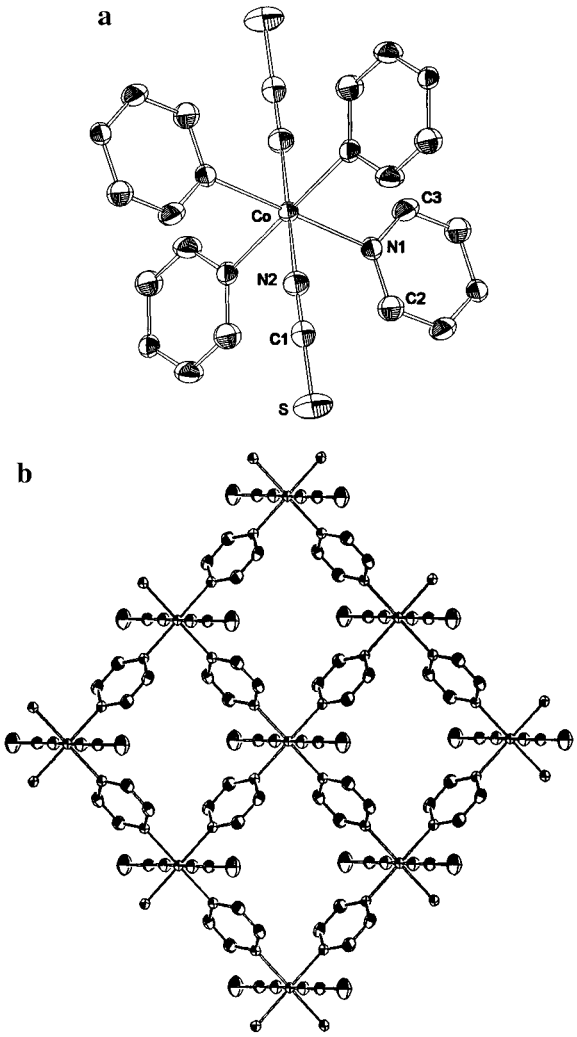

Figure 1. (a) Ortep drawing of the local coordination of Co in **1** with thermal ellipsoids at the 50% probability level. (b) Extended structure of **1**.

Å. Locally, Co sits on a 2/*m* site and a mirror plane passes through NCS. Co is in a compressed octahedral environment with four long Co−N (pyrazine) bonds (2.210(2) Å) and two short Co−N (NCS) bonds (2.050(3) Å). The pyrazine ring is canted to the Co−N4 plane at an angle of 64°. The NCS group is almost linear with an N−C−S angle of 178.0(3)°. The connection between Co atoms and NCS groups are bent with a C(1)−N(2)−Co angle of 158.8(3)°.

In **2**, two water molecules in addition to the NCS groups are directly coordinated to the cobalt centers. **2** is isostructural with $Mn(NCS)_2(H_2O)_2$(4,4′-bipy)·4,4′-bipy.[22] The cobalt centers are bridged by 4,4′-bipy ligands, resulting in the formation of a linear Co−bipy−Co chain. As in **1**, the NCS groups occupy terminal positions (Figure 2a). A second type of 4,4′-bipy molecule is hydrogen-bonded (2.74 Å) to the coordinated water molecules and connects adjacent chains (Figure 2b). Linear Co−bipy−Co chains and zigzag Co−H_2O-bipy-H_2O−Co chains form a stair type connection. These stair type layers alternate similarly to the layers in **1**, so that the cobalt center in an adjacent layer is above or below the center of the rectangles formed by Co−bipy−Co and Co−H_2O-bipy-H_2O−Co chains. The two pyridine rings are coplanar in both the coordinated and hydrogen-bonded types of 4,4′-bipy ligands. No obvious overlap between pyridine rings is observed. Other examples

(22) Li, M. X.; Xie, G. Y.; Gu, Y. D.; Chen, J.; Zheng, P. J. *Polyhedron* **1995**, *14*, 1235.

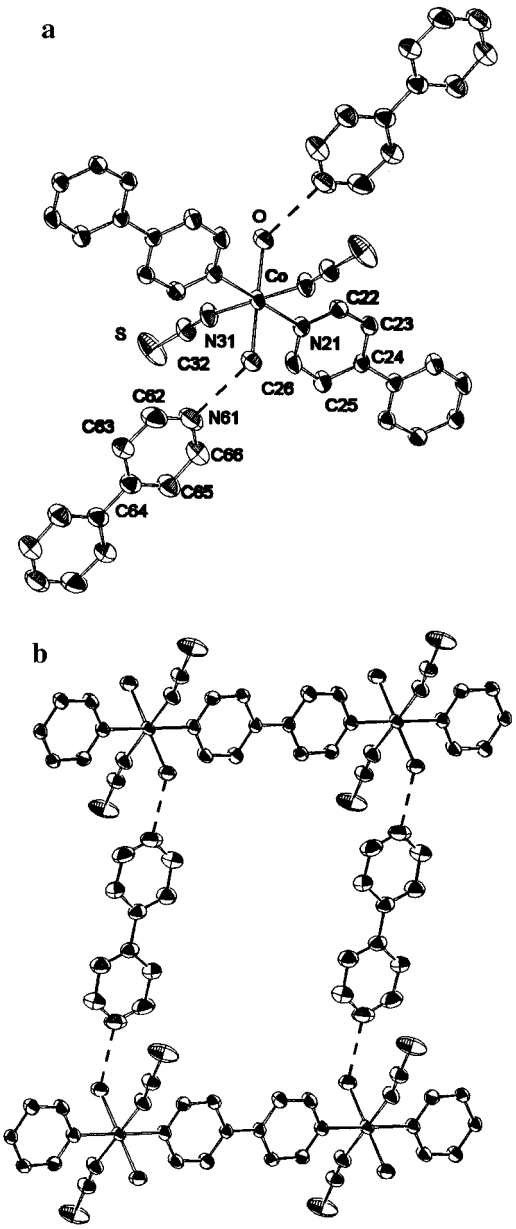

Figure 2. (a) Ortep drawing of the local coordination of Co in **2** with thermal ellipsoids at the 50% probability level. (b) Extended structure of **2**. Dotted lines indicate hydrogen bonding.

of coordination polymers with coplanar 4,4′-bipy units include $Zn(4,4'\text{-bipy})_2(H_2O)_2SiF_6$[6] and $Zn(4,4'\text{-bipy})_2SiF_6$.[7] Locally, Co sits on the $\bar{1}$ position and the coordination around Co is an elongated octahedron. There are two short Co−O (H_2O) bonds (2.096(2) Å), two short Co−N (NCS) bonds (2.095(2) Å), and two long Co−N (bipy) bonds (2.162(2) Å). The NCS group is almost linear (N−C−S = 178.6(3)°). The bonds between the NCS groups and the Co atoms are more nearly linear (C(32)−N(31)−Co = 168.9(2)°) than in **1**.

The structure of $Mn(NCS)_2(H_2O)_2$(4,4′-bipy)·4,4′-bipy was apparently solved in space group $P1$[22] according to the asymmetric unit contents and the number of parameters refined even though space group $P\bar{1}$ was used in the crystallographic data table. In the case of **2**, we found that $P\bar{1}$ is the correct choice and there are large correlations between inversion-center-related atoms if the structure is refined in $P1$. The bond distances and bond angles in **2** and $Mn(NCS)_2(H_2O)_2$(4,4′-bipy)·4,4′-bipy are the same within the experimental errors except for distances involving the metal centers. The metal to oxygen (water) and nitrogen (NCS or bipy) distances are noticeably longer in

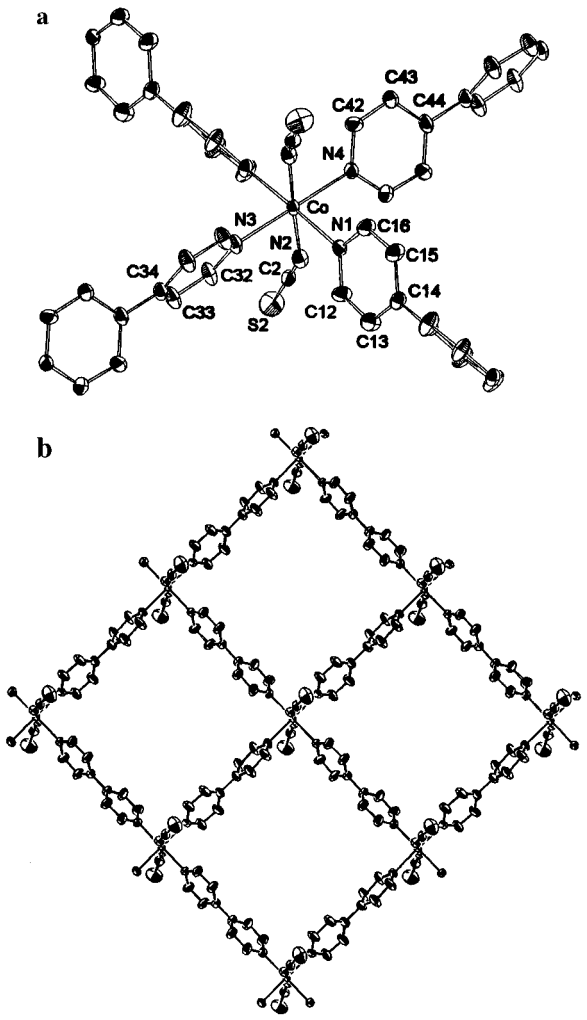

Figure 3. (a) Ortep drawing of the local coordination of Co in **3** with thermal ellipsoids at the 30% probability level. (b) Extended structure of **3**.

$Mn(NCS)_2(H_2O)_2$(4,4′-bipy)·4,4′-bipy than in **2** (average Mn−O = 2.198 Å vs Co−O = 2.096(2) Å; average Mn−N (NCS) = 2.175 Å vs Co−N (NCS) = 2.095(2) Å; average Mn−N (bipy) = 2.278 Å vs Co−N (bipy) = 2.162(2) Å). The Co−O and Co−N distances in **2** are comparable to those in the related structures (e.g.: Co−O (H_2O) = 2.10(4) Å in $CoSO_4$·pyz·$6H_2O$;[23] average Co−N (vinylpyridine) = 2.17 Å in $Co(NCS)_2$-(4-vinylpyridine)$_4$[24]).

The structure of **3** is similar to that of **1**. The 4,4′-bipy ligands bridge cobalt(II) centers, and the NCS groups are terminal ligands. The structure of **3** is a 2D network. Figure 3 shows the local coordination of cobalt ions and a view of the extended structure of **3**. The Co−bipy layers are staggered relative to each other so that the Co atoms in one layer sit above or below the squares formed by the cobalt atoms of the adjacent layers. Layers stack along the *c* axis, and the distance between layers is 6.49 Å. This separation distance falls in the range (6.28−7.01 Å) observed in related compounds.[11b,11c,16,20] In contrast to the arrangement in **2**, in **3** the two pyridine rings of the bipy molecule are not coplanar. The bipyridine dihedral angle is 56°. Also in contrast to **2**, the solvent molecules (in this case, ether) occupy voids in the lattice rather than being coordinated directly to the metal centers. Locally, Co is in a compressed octahedron with four long Co−N (bipy) bonds (2.164−2.199 Å) and two short Co−N (NCS) bonds (2.076 Å). A 2-fold axis passes through Co−N4−C44−C34−N3. The NCS group is almost linear with a N−C−S angle of 178.4(4)°. The connection between Co atoms and NCS groups are bent with C(1)−N(2)−Co angle of 153.2(3)°. In all three compounds, the NCS groups have almost linear N−C−S connections but differ in the Co−N−C angles. The Co−N−C angles are noticeably smaller in **1** and **3** (158.8(3) and 153.2(3)°) than in **2** (168.9(2)°). The smaller Co−NCS angle in **1** and **3** results in closer interlayer distances and more effective packing of the layers.

Only a small number of two-dimensional coordination polymers in which 4,4′-bipyridine ligands bridge metal centers have been reported. Several of these structures contain binuclear copper centers bridged by additional ligands, for example carboxylate.[4c,25] Other known structures that contain single metal centers bridged by 4,4′-bipy ligands can be classified into those forming square nets (e.g., $Zn(4,4'\text{-bipy})_2SiF_6$,[7] $Cd(H_2O)_2$-$(4,4'\text{-bipy})_2(PF_6)_2$·$2(4,4'\text{-bipy})$·$4H_2O$,[5a] and $[Cd(4,4'\text{-bipy})_2]$-$(NO_3)_2$·$2C_6H_4Br_2$[16]) and those with interpenetrating square nets (e.g., $M(4,4'\text{-bipy})_2(H_2O)_2SiF_6$ (M = Zn, Cu, Cd)[5a,6] and $Cd(H_2O)(OH)(4,4'\text{-bipy})_2PF_6$[5a]).

The structures of **3** and $[Cd(4,4'\text{-bipy})_2](NO_3)_2$·$2C_6H_4Br_2$[16] are related. Both structures contain two-dimensional square nets of composition $^2_\infty[M(4,4'\text{-bipy})_{4/2}]$ that do not interpenetrate. In the structure of the Cd compound, the included $C_6H_4Br_2$ solvent molecules interact with the host lattice with the result that the pyridine rings in one type of 4,4′-bipyridine ligand are coplanar. In **3**, the interactions with the solvent (ether) molecules are much weaker and the pyridine rings adopt a sterically more favorable non-coplanar arrangement. The structures of $Zn(4,4'\text{-bipy})_2SiF_6$[7] and $Cu(pyz)_2NbOF_5(pyz)$-(H_2O)[11a] are also related to that of **3**. They have the same $^2_\infty[ML_{4/2}]$ 2D net, but adjacent layers are cross-linked by bridging SiF_6^{2-} or $[NbOF_5]^{2-}$ anions to form three-dimensional lattices. Since there is no apparent interaction between the ether molecules and the host lattice in **3**, the reason that **3** does not form an interpenetrating structure is unclear.

Unlike the structure of $Zn(4,4'\text{-bipy})_2(H_2O)_2SiF_6$,[6] the structure of **2** is not interpenetrating. The structure can be described as a nonplanar two-dimensional lattice but with the connections in one direction formed by hydrogen bonds between 4,4′-bipy and the coordinated water molecules. If the metric difference between the two orthogonal directions is ignored, then the structure is related to the nonplanar 2D square net formed by $[Ag(pyz)_2](PF_6)$.[9]

Reaction Chemistry. The nature of products obtained from the reactions of $Co(NCS)_2$ with pyrazine and 4,4′-bipyridine depends on the specific solvent used. Although $Co(NCS)_2$ reacts with pyrazine to give only one product in different solvents (as shown by X-ray powder diffraction data), the quality of the crystals formed varies. The best single crystals of $Co(NCS)_2$-$(pyz)_2$ were obtained by interdiffusion of $Co(NCS)_2$ dissolved in water and pyrazine dissolved in acetone. Other solvent combinations, for example, water/THF, water/EtOH, water/CH_3CN, and water/MeOH, gave single-phase microcrystalline material.

The products from the reaction of $Co(NCS)_2$ with 4,4′-bipy are different in different solvent systems. Orange crystals of **2** are formed from a H_2O ($Co(NCS)_2$)/EtOH (4,4′-bipy) system. If ether is used in place of ethanol, two types of crystals are formed in the same tube. Orange-red square crystals of **3** form at the solution interface, and orange crystals of **2** appear farther

(23) Fetzer, Th.; Jooss, R.; Lentz, A.; Debaerdemaeker, T. *Z. Anorg. Allg. Chem.* **1994**, *620*, 1750.
(24) Foxman, B. M.; Mazurek, H. *Inorg. Chim. Acta* **1982**, *59*, 231.
(25) (a) Chen, Z. N.; Fu, D. G.; Yu, K. B.; Tang, W. X. *J. Chem. Soc., Dalton Trans.* **1994**, 1917. (b) Liu, S. X. *Acta Crystallogr.* **1992**, *C48*, 22.

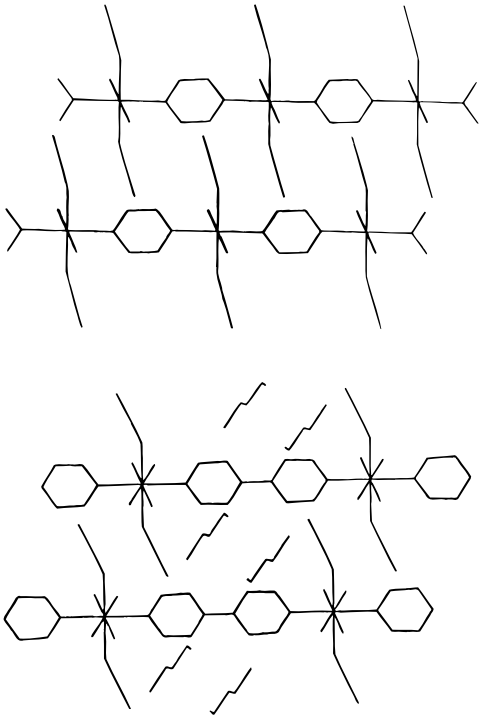

Figure 4. (a) Structure of **1** viewed down the *b* axis. (b) Structure of **3** viewed down the *b* axis. Ether molecules occupy the space between the layers.

down in the reaction tube. When water is eliminated from the system by using, for example, an EtOH/ether combination, only compound **3** forms.

As can be seen by comparison of the structures of **1** and **3** (see Figure 4), changing the bridging ligand from pyrazine to 4,4′-bipy increases the empty space in the lattice. The extra space is occupied by solvent, in this case ether molecules.

Unlike the $AgBF_4$/pyrazine system, changing the stoichiometry does not change the nature of the final products.

Thermogravimetric Analysis. **1**, **2**, and **3** were heated to 350 °C in N_2 (Figure 5). For **1**, TGA showed a weight loss corresponding to one pyrazine (observed 23.82%, calculated 23.88%) in the temperature range 170−260 °C, immediately followed by another weight loss corresponding to one pyrazine molecule (observed 23.80%, calculated 23.88%) from 260 to 310 °C. The weight loss continued above 310 °C and the final residue was black and amorphous.

The thermal decomposition behavior of **2** is much like that reported for $Mn(NCS)_2(H_2O)_2(4,4'\text{-bipy})\cdot 4,4'\text{-bipy}$.[22] The TGA data for **2** showed two separate weight losses. First, the sample lost weight corresponding to two water molecules (observed 6.88%, calculated 6.88%) from 70 to 130 °C. A light orange crystalline material (**2a**) was formed. The X-ray powder diffraction pattern of **2a** is identical to the X-ray pattern of **3** after loss of the ether molecules (see below, **3a**). On further heating, **2a** lost weight between 140 and 250 °C corresponding to one molecule of bipy (observed 29.52%, calculated 29.83%). The residue at this stage was a violet crystalline material (**2b**) which gave a sharp though complex powder diffraction pattern. Further weight loss was observed when **2b** was heated above 270 °C with contiguous loss of another molecule of bipy and decomposition of $Co(NCS)_2$. The final residue at 350 °C was black and amorphous.

3 lost ether (**3a**) immediately after the crystals were removed from the mother liquor. **3a** has an X-ray powder pattern identical to that of **2a** and shows the same thermal decomposition pattern as that of **2a**. One molecule of bipy is lost between

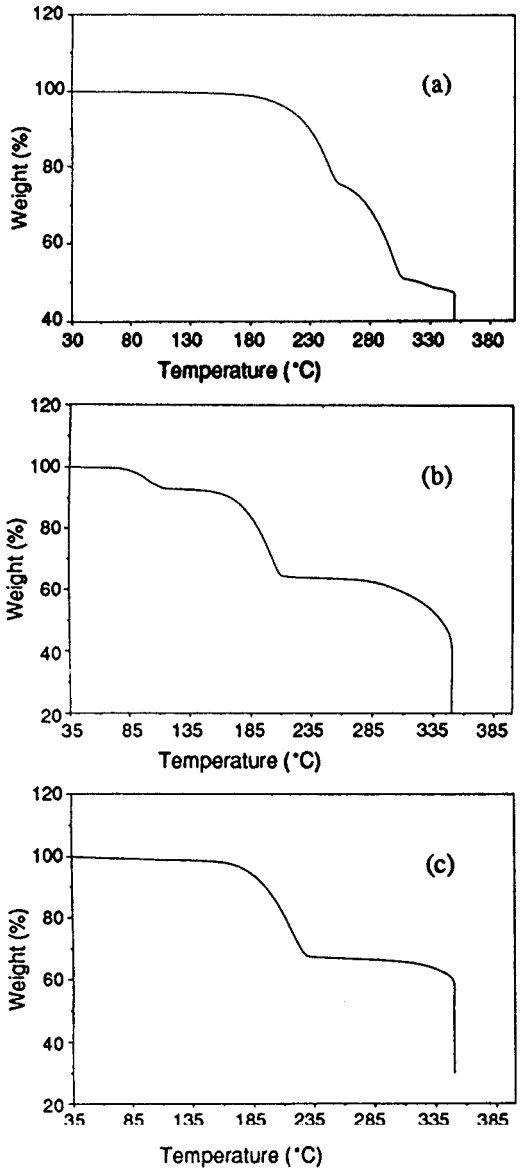

Figure 5. Thermogravimetric analysis data for (a) **1**, (b) **2**, and (c) **3**.

140 and 250 °C to give violet crystalline material (**3b**) with a powder pattern identical to that of **2b**.

The TGA results for **2** and **3** can be summarized as follows:

$$Co(NCS)_2(H_2O)_2(4,4'\text{-bipy})\cdot 4,4'\text{-bipy} \xrightarrow[70\text{ - }130\ ^\circ C]{-\,2H_2O} Co(NCS)_2(4,4'\text{-bipy})_2 \xrightarrow[140\text{ - }250\ ^\circ C]{-\,bipy}$$

$$Co(NCS)_2(4,4'\text{-bipy}) \xrightarrow[>\,270\ ^\circ C]{} \text{further decomp.}$$

$$Co(NCS)_2(4,4'\text{-bipy})_2\cdot 2(CH_3CH_2)_2O \xrightarrow[25\ ^\circ C]{-\,2(CH_3CH_2)_2O} Co(NCS)_2(4,4'\text{-bipy})_2 \xrightarrow[140\text{ - }250\ ^\circ C]{-\,bipy}$$

$$Co(NCS)_2(4,4'\text{-bipy}) \xrightarrow[>\,270\ ^\circ C]{} \text{further decomp.}$$

The intermediates in the decomposition of **1** were not followed by X-ray powder diffraction, since the loss of pyrazine molecules did not occur in discrete steps.

The X-ray powder diffraction data indicate that the intermediate crystalline compounds **2a**/**3a** and **2b**/**3b** have closely similar structures. Proposed structures for the intermediate phases are shown in Scheme 1. The structures of **2a** and **3a** are derived from the structure of **3** by loss of ether molecules but with retention of the layers. The structural transformation from **2**

Scheme 1. Thermal Decomposition of **2** and **3** and the Proposed Structures of the Intermediates

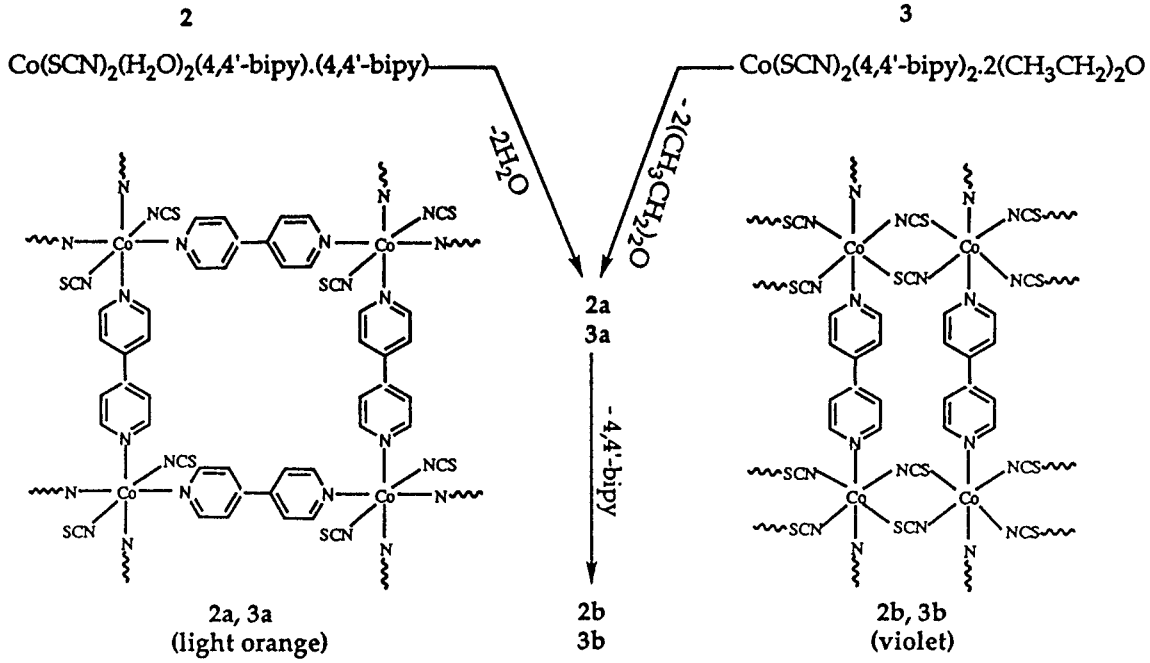

to **2a** is also suggested by the extended structure of **2** (Figure 2b). The bipy molecules are aligned such that they can readily connect to the metal centers on elimination of two water molecules. The conformation of the pyridine rings probably changes so that the two pyridine rings are no longer coplanar as in **3**. The first 4,4′-bipyridine loss in **2** occurs at relatively low temperature (140−250 °C). Coordinated pyridine ligands are removed thermally at comparably low temperatures in $Co(4\text{-vinylpyridine})_4(NCS)_2$ (115 °C).[24] The light orange color of **2a** suggests that, after losing the water molecules, the Co^{2+} centers remain octahedrally coordinated. The identical X-ray powder patterns of **2a** and **3a** further suggest that all 4,4′-bipyridine ligands are coordinated to Co(II) centers.

The thermal decomposition of metal halogen or pseudohalogen compounds containing substituted pyridine ligands results in blue or violet compounds.[24] In the case of $Co(4\text{-vinylpyridine})_2Cl_2$, the structures of both blue and violet forms have been determined.[26,27] In the blue form, cobalt ions are tetrahedrally coordinated,[26] while in the violet form, they are octahedrally coordinated *via* bridging chlorine atoms.[27] The thermal decomposition products **2b** and **3b** are violet, suggesting octahedral coordination. In order to maintain octahedral coordination at cobalt centers after the loss of one bipy molecule, the NCS groups must become bridging rather than terminal. The *trans* arrangement of bipy ligands (Scheme 1) is chosen on the basis of the structures of $Co(py)_2(NCS)_2$[28] and $Cu(py)_2(NCS)_2$.[29] This structure type is also seen in $MX_2(4,4'\text{-bipy})$ ($M = Ni^{2+}$, Cu^{2+}; X = Cl, Br)[30] and $Cu(pyz)X_2$ (X = Cl, Br).[31]

Conclusions

Three new coordination polymers formed by $Co(NCS)_2$ with the bridging ligand pyrazine or 4,4′-bipyridine have been prepared and characterized. As in other systems, we observe that solvent plays an important role in the crystallization process and solvent coordination or solvent inclusion determines the final polymer structure. None of the three compounds form interpenetrating lattices. Future work involves the determination of the magnetic properties and the extension to 3D structures by bridging adjacent layers through the NCS groups. We are also investigating the effect in the Co−bipy system of the counterions. In $Co(NO_3)_2(4,4'\text{-bipy})(H_2O)_3\cdot 2H_2O$, NO_3^- and SO_4^{2-} directly coordinate to Co centers and form chain structures.[32] Cobalt analogs of $Zn(4,4'\text{-bipy})_2(H_2O)_2SiF_6$ and $Zn(4,4'\text{-bipy})_2SiF_6$ have also be synthesized.[32]

Acknowledgment. We thank the Texas Advanced Research Program (Grant No. 003652-048), the National Science Foundation (Grant No. DMR-9214804), and the Robert A. Welch Foundation for financial support.

Supporting Information Available: Listings of detailed crystallographic data, complete tables of bond distances and angles, and tables of anisotropic thermal parameters (13 pages). Ordering information is given on any current masthead page.

IC961158G

(26) Admiraal, L. J.; Gafner, G. *Chem. Commun.* **1968**, 1221.
(27) Laing, M.; Horsfield, E. *Chem. Commun.* **1969**, 902.
(28) Poraj-Kosic, M. A.; Tiscenko, G. N. *Kristallografiya* **1959**, *4*, 239.
(29) Soldanova, J.; Kabesova, M.; Gazo, J. *Inorg. Chim. Acta* **1983**, *76*, L203.
(30) Masciocchi, N.; Cairati, P.; Carlucci, L.; Mezza, G.; Ciani, G.; Sironi, A. *J. Chem. Soc., Dalton Trans.* **1996**, 2739.
(31) Fetzer, Th.; Lentz, A.; Debaerdemaeker, T. *Z. Naturforsch.* **1989**, *44B*, 553.
(32) Lu, J.; Niu, T.; Jacobson, A. J. To be published.